

Correlating seabird movements with ocean winds: linking satellite telemetry with ocean scatterometry

Josh Adams · Stephanie Flora

Received: 23 February 2009 / Accepted: 1 December 2009 / Published online: 29 December 2009
© Springer-Verlag 2009

Abstract Satellite telemetry studies of the movements of seabirds are now common and have revealed impressive flight capabilities and extensive distributions among individuals and species at sea. Linking seabird movements with environmental conditions over vast expanses of the world's open ocean, however, remains difficult. Seabirds of the order Procellariiformes (e.g., petrels, albatrosses, and shearwaters) depend largely on wind and wave energy for efficient flight. We present a new method for quantifying the movements of far-ranging seabirds in relation to ocean winds measured by the SeaWinds scatterometer onboard the QuikSCAT satellite. We apply vector correlation (as defined by Crosby et al. in *J Atm Ocean Tech* 10:355–367, 1993) to evaluate how the trajectories (ground speed and direction) for five procellariiform seabirds outfitted with satellite transmitters are related to ocean winds. Individual seabirds (Sooty Shearwater, Pink-footed Shearwater, Hawaiian Petrel, Grey-faced Petrel, and Black-footed Albatross) all traveled predominantly with oblique,

isotropic crossing to quartering tail-winds (i.e., 105–165° in relation to birds' trajectory). For all five seabirds, entire track line trajectories were significantly correlated with co-located winds. Greatest correlations along 8-day path segments were related to wind patterns during birds' directed, long-range migration (Sooty Shearwater) as well as movements associated with mega-scale meteorological phenomena, including Pacific Basin anticyclones (Hawaiian Petrel, Grey-faced Petrel) and eastward-propagating north Pacific cyclones (Black-footed Albatross). Wind strength and direction are important factors related to the overall movements that delineate the distribution of petrels at sea. We suggest that vector correlation can be used to quantify movements for any marine vertebrate when tracking and environmental data (winds or currents) are of sufficient quality and sample size. Vector correlation coefficients can then be used to assess population—or species-specific variability and used to test specific hypotheses related to how animal movements are associated with fluid environments.

Communicated by S. Garthe.

J. Adams (✉)
US Geological Survey, Western Ecological Research Center,
Moss Landing Marine Laboratories, 8272 Moss Landing Road,
Moss Landing, CA 95039, USA
e-mail: josh_adams@usgs.gov

S. Flora
Physical Oceanography Laboratory,
Moss Landing Marine Laboratories,
Moss Landing, CA, USA

Present Address:

J. Adams
Department of Zoology, University of Otago,
Dunedin, New Zealand

Introduction

Marine vertebrates, including fish, turtles, pinnipeds, cetaceans, and seabirds, exist within a turbulent environment of ocean currents and near-surface winds (Schneider 1991). At sea, seabirds of the order Procellariiformes (e.g., petrels: gadfly petrels, shearwaters, and albatrosses) dwell between the wave-roughened surfaces of the oceans and the lower ~30 m of the atmosphere (Wilson 1975; Alerstam et al. 1993; Pennycuick 2002). Because petrels have evolved flight characteristics that allow them to extract energy from prevailing winds over the ocean's surface—variability in wind speed and direction encountered by birds is of

fundamental importance (Ainley 1977; Furness and Bryant 1996; Ballance et al. 1997; Spear and Ainley 1998; Weimerskirch et al. 2000; Shaffer et al. 2001a, b; Phillips et al. 2004; Spear et al. 2007). Wind is particularly important for petrels that have large ranges at sea (millions of square kilometers), foraging trips that can exceed thousands of kilometers during the breeding season (Jouventin and Weimerskirch 1990; Phalan et al. 2007; MacLeod et al. 2008), and long-distance trans-oceanic migrations (Spear and Ainley 1999; Croxall et al. 2005; Shaffer et al. 2006). Such impressive ranging behaviors are determined in part by wing morphology (Warham 1977; Pennycuick 1982; Spear and Ainley 1997a; Weimerskirch et al. 2000) and flight behavior according to prevailing wind conditions (Pennycuick 2002; Sachs 2005).

In recent decades, meteorologists and oceanographers have developed remote sensing technologies (e.g., scatterometry, radar altimetry) and models to depict global atmospheric and oceanographic circulation patterns (Kalnay et al. 1996; Kistler et al. 2001). At the same time, ecologists increasingly have used tracking devices attached to seabirds to measure movements over large regions of the world's oceans (e.g., satellite transmitters, global positioning systems, and archival geolocation sensors; Burger and Shaffer 2008; Phillips et al. 2008). Given advances in device miniaturization, it is now possible to track even the fine-scale movements of small-bodied (<1,000 g) seabirds throughout the world's oceans. Obtaining linked environmental information at sea, however, remains challenging (Wilson et al. 2002).

Linking flight behaviors and movements at sea to wind speed and direction is required for understanding aspects of foraging ecology especially among far-ranging seabirds. Both the direction and velocity of wind must be considered to determine the amount of power (and thus energy) required in the various modes of flight. Previous studies have focused on direct observations and mathematical modeling of flight behaviors. For example, Pennycuick (1982, 1997, 2002) quantified flight behaviors among a variety of petrels and calculated 'minimum power' speeds and 'maximum range' speeds. And in the southern Atlantic, Alerstam et al. (1993) observed albatrosses adjusted their mean flight directions with respect to wind direction according to wind speed. Presently, however, we are not aware of any previous avian study that has applied a technique that can generate a singular mathematical test statistic (e.g., correlation coefficient) that relates seabird flight directions and speeds to ocean winds. Such application could potentially allow more refined statistical hypotheses testing or improve modeling approaches (Felicísimo et al. 2008; González-Solís et al. 2009). A better understanding of how seabirds travel in association with winds also is important for the interpretation of

distributional patterns at sea recorded from ships (Abrams 1985; Spruzen and Woehler 2002) and may prove useful, following sufficient ground-truthing, for correction of at-sea densities based on movements relative to winds and ship direction (Spear et al. 1992).

Herein, we apply vector correlation (Crosby et al. 1993) to quantify the association of seabird movements at sea with ocean winds. First, we provide an example of vector correlation applied to satellite-bourn, scatterometer-derived winds (SeaWinds on QuikSCAT, hereafter QSCAT), and continuous winds recorded by six meteorological buoys in the North Pacific Ocean. In this example, we expect vector correlations to be relatively high because the two platforms are independent measures of the same phenomenon, ocean winds. This example primarily is for proof of concept and secondarily to address how our purpose-built programs attempt to confront certain aspects of anticipated variability in QSCAT data such as near-coastal measurements of winds and potential effects of small-scale weather phenomena. Second, based on previous observations (Alerstam et al. 1993; Weimerskirch et al. 1993; Spear and Ainley 1997a, b), we hypothesize that movements (i.e., path segments) that comprise individual track lines among five satellite-tracked petrels are correlated with wind speed and direction measured by QSCAT over the open ocean. Furthermore, the petrels in this study should fly predominantly with quartering tail-winds (i.e., 105–165° with respect to birds' trajectories).¹

Methods

Vector correlation

Meteorologists and oceanographers seeking to quantify wind and current patterns developed vector correlation to measure the degree of association between two independent sets of vectors. Detailed reviews and mathematical proofs for vector correlation are presented in Breckling (1989) who reviewed angle and direction correlation; Hanson et al. (1992) provided a meteorological application; and Crosby et al. (1993) present the necessary background describing the basic mathematical properties of vectors, properties of the product-moment correlation coefficient, and a brief history of vector correlation. Crosby et al. (1993) suggested a "universally acceptable" definition of vector correlation for geophysics with an example evaluating coherence among marine surface winds. Recently,

¹ We consider the incidental angle of the wind as it touches a bird traveling in the forward direction such that wind angles 105–165° are equivalent to winds 195–255°; throughout, we refer to the incidental angles between 0 and 180° a convention that is independent of left-versus right-lateral incidence. See Fig. 4 for a graphical explanation.

vector correlation has been used to cross-validate winds measured at oceanographic buoys with winds derived using satellite scatterometry (Freilich and Dunbar 1999), patterns and dynamics of coastal breezes off the west coast of India (Aparna et al. 2005), and the relationship between synoptic winds and currents in the Santa Barbara Channel, CA (Breaker et al. 2003). We are aware of only three biological studies that have used vector correlation: Acosta et al. (1997) used complex vector correlation (Kundu 1976) to assess post-larval recruitment of spiny lobster (*Panulirus argus*) as related to wind forcing; Queiroga (2003) examined the same dynamic for crab megalopae (*Carcinus maenas*); and Brooks (2005) evaluated tidally influenced movements of green sea turtles (*Chelonia midas*) in a channelized estuary following Crosby et al. (1993).

For our purposes, consider the two-dimensional vector \mathbf{W} in earth-oriented Cartesian coordinates such that component u increases to the right (eastward) along the x -axis and v increases upward (northward) along the y -axis. Analytical methods required for vectors need to account for both magnitude and direction. The generalized correlation coefficient (ρ_v^2) of Crosby et al. (1993) is based on mathematics described in Hooper (1959) and the complex correlation coefficient (ρ_T) of Kundu (1976). Both coefficients (ρ_v^2 and ρ_T) provide simple, scalar statistical measures of the degree of agreement between two, two-dimensional vector series. Because covariances of both scalar components (u and v) of each vector are considered, the single generalized correlation coefficient accounts for the contribution of both components toward the overall correlation. The coefficient ρ_v^2 ranges from 0 to 2, with 2 indicating perfect agreement between the two vector sets. The technique is invariant to coordinate system transformations and scaling applied to either vector data set by a constant magnitude or angular shift. Empirical tests by Crosby et al. (1993) showed that for sample sizes >64 , the distribution of nr_v^2 , where n = the sample size used to calculate r_v^2 (the corresponding sample parameter for the population parameter ρ_v^2) approximates the theoretical chi-square

distribution with four degrees of freedom. This property and graphical presentation of bootstrap estimates for smaller sample sizes (as few as $n = 8$) allow for vector correlation significance tests at various sample sizes (Crosby et al. 1993; Breaker et al. 1994).

Wind speed and direction: oceanographic buoys and QuikSCAT scatterometry

We obtained continuous wind speed and direction data (10 min vector averaged) from six National Data Buoy Center (NDBC) moored buoys located throughout the eastern north Pacific (Table 1). Anemometers at all buoys recorded continuous wind speed (ms^{-1}) and *blow* direction (i.e., meteorological convention, where a wind direction of 0° implies a wind *blowing* from the north, e.g., a *northerly* wind). We used hourly averaged 10 min winds (NDBC 2003) and adjusted wind speeds to 10-m-equivalent neutral stability winds following Liu and Tang (1996). We obtained wind speed and direction data derived from the SeaWinds microwave scatterometer instrument flown on the QuikSCAT spacecraft (QSCAT; Jet Propulsion Laboratory [JPL] 2006) from remote sensing systems (RSS, Santa Rosa, California, www.remss.com, accessed October 14, 2009). The QSCAT satellite follows a sun-synchronous orbit and scans an 1,800-km-wide swath of the Earth's surface such that approximately 90% of the Earth's surface is scanned daily; ocean winds are measured at approximately 0600 local time (ascending pass) and 1800 (descending pass). Root-mean-squared differences between buoy and QSCAT winds are 1.01 ms^{-1} for magnitude and 23° for direction (Ebuchi et al. 2002) with a spatial resolution of 25–50 km (Freilich and Dunbar 1999; JPL 2006). In a comparison between land-based stations and QSCAT winds, Sánchez et al. (2007) report coherence in wind measurements could exceed 150 km in areas where land and coastal effects on wind fields and wave reflection are minimal (i.e., the open ocean far from land effects). We used RSS Version 3 gridded bytemap files ($0.25^\circ \times 0.25^\circ$

Table 1 Summary of wind data at six National Data Buoy Center (NDBC) locations throughout the northeast Pacific and co-located synoptic winds derived from the SeaWinds scatterometer onboard the QuikSCAT spacecraft

Buoy	Location	Latitude	Longitude	Year	Days available (%)	Total # co-locations	# rain flagged (%)	# wind flagged (%)	# co-locations retained (%)
46063	Point Conception, CA	34.27°	−120.70°	2005	60 (16)	99	8 (8)	13 (13)	78 (79)
46066	Southern Aleutians, AK	52.70°	−154.98°	2005	209 (57)	435	14 (3)	42 (10)	381 (88)
46042	Monterey Bay, CA	36.75°	−122.42°	2006	365 (100)	626	104 (17)	66 (11)	469 (75)
46059	Offshore CA	37.98°	−130.00°	2006	365 (100)	655	30 (5)	46 (7)	588 (90)
51004	Southeast HI	17.59°	−152.46°	2006	365 (100)	534	17 (3)	31 (6)	492 (92)
51028	Christmas Island	0°	−153.89°	2006	365 (100)	513	6 (1)	37 (7)	471 (92)

pixel resolution; $27.8 \text{ km} \times 27.8 \text{ km}$, 773 km^2) of wind speed (ms^{-1} at a 10-m adopted reference height) and flow direction (i.e., oceanographic convention, where a current or wind direction of 0° implies *flowing* toward the north, e.g., a *northward* wind). RSS QSCAT wind direction data conventions are 180° reversed from NDBC buoy wind direction data. RSS Version 3 data incorporate the Ku-2001 geophysical model function and use a more strict rain contamination flagging based on additional sensor measurements (JPL 2006). We used Matlab (MathWorks 2007) scripts (available via RSS web site) to archive ascending and descending QSCAT wind speed and direction data. We used purpose-built Matlab programs to match buoy winds and synoptic petrel locations with QSCAT winds based on swath-coverage-times for the satellite as it passed over each buoy (or petrel) location a maximum of twice daily (co-locations). We defined co-located QSCAT wind data as the pixel containing the buoy's (or petrel's) location. Before analyses, we removed potentially contaminated QSCAT data (indicated by a rain flag in the data provided by RSS). In addition, because QSCAT winds occasionally are reversed (i.e., rotated 180° , most frequently during low-wind conditions) and can be spatially variable near the coast, we evaluated the directional standard deviation (SD_{dir}) using a “single-pass” estimator technique (Yamartino 1984) for wind directions within a QSCAT 3×3 -pixel window centered on co-located pixel. We excluded QSCAT data from analyses when SD_{dir} was greater than $2 \times$ overall mean SD_{dir} for all windows in the data set. If co-located pixels did not have wind data or were flagged, we selected the closest adjacent pixel data with a maximum distance and time cut-offs of 19.4 km and 2 h. We considered this cutoff to be appropriate because the distance is within the range of coherent winds described in previous validation studies (Freilich and Dunbar 1999; JPL 2006; Sánchez et al. 2007).

Satellite telemetry of five petrel species

We arbitrarily selected one individual each from five different species' tracking data sets for analyses: Sooty Shearwater (SOSH, *Puffinus griseus*), Pink-footed Shearwater (PFSH, *Puffinus creatopus*), Hawaiian Petrel (HAPE, *Pterodroma sandwichensis*), Grey-faced Petrel (GFPE, *Pterodroma macroptera gouldi*), and Black-footed Albatross (BLAL, *Phoebastria nigripes*). We outfitted individuals with satellite-linked platform terminal transmitters (PTTs) programmed with 60-s repetition rates and duty cycles that ranged from continuous (i.e., no off period; HAPE, SOSH, BFAL), 2 h on:2 h off (GFPE), and 10 h on:48 h off (PFSH). We attached PTTs along the dorsal midline between the scapulae following MacLeod et al. (2008) and Hyrenbach et al. (2002; BFAL). Bird locations

were generated by CLS-ARGOS (CLS 2007), and we retained data for location classes (LC) 3, 2, 1, 0, A, and B and excluded all unclassified locations (i.e., LC Z). We used satellite tracking and analyses tools (STAT) online software (Coyne and Godley 2005, www.seaturtle.org/STAT, accessed October 14, 2009) to manage and pre-filter ARGOS data. First, STAT flagged potential “swapped locations” (for each location generated, ARGOS reports two sets of latitude and longitude coordinates [“mirror locations”], and occasionally set two contains the more accurate location). We examined mirror locations and these were manually swapped if needed. Second, when ARGOS returned two sets of location data for the same time, we selected the location with the more accurate LC, or greater number of uplinks received by satellites. We exported pre-filtered data from STAT for final filtering using the publically available R package *argosfilter* version 0.5 (R Development Core Team 2007; Freitas et al. 2008, <http://cran.r-project.org/web/packages/argosfilter/index.html>, accessed October 14, 2009). We used *SDA filter* (Freitas et al. 2008) with speed, distance, and angle (SDA) criteria to remove imprecise ARGOS location data. We modified the scripting to allow a maximum threshold speed for filtering of 70 km h^{-1} , and applied default minimum and maximum angle and distance values set at 15° and 2,500 m, and 25° and 5,000 m, respectively, for all individuals. We then interpolated filtered data using Matlab to hourly locations using the linear technique of Tremblay et al. (2006). We avoided generating interpolated locations between ARGOS locations separated by >8 -h. We used the interpolated, hourly bird location data to generate a bird-movement vector set (\mathbf{W}_2 ; i.e., bearing and speed, oceanographic convention) and decomposed these to \mathbf{u} and \mathbf{v} scalar components of bird movements.

Vector correlations of (1) winds measured at buoys and (2) seabird movements with winds measured by QuikSCAT scatterometry

First, we used vector correlation following Crosby et al. (1993) to evaluate the degree of association between buoy and co-located QSCAT winds. Similar to other studies having analogous objectives (i.e., validation and assessment of QSCAT winds), this exercise allowed us to evaluate our purpose-built programs within a context where we expected high and statistically significant vector correlations. We determined statistical significance among vector correlation coefficients r_v^2 by randomly sampling (with replacement) paired vector sets from buoy data and shuffled QSCAT data. For each of 10,000 permutations, we calculated the vector correlation coefficient r_v^2 and determined probability values for r_v^2 by summing the number of permuted r_v^2 values \geq the

empirical value, divided by 10,000. Statistical significance for r_v^2 was determined by setting $\alpha = 0.05$ (Breaker et al. 1994).

Secondly, we used vector correlation to evaluate the degree of association between seabird flight trajectories (speed and direction) and co-located QSCAT winds. We matched bird-movement data to daily QSCAT wind data (W_1) according to the bird's synoptic position with QSCAT satellite over-passes (using QSCAT swath-coverage-times as described earlier). Nicholls and Robertson (2007) contributed lengthy discussion regarding the estimation of speeds using ARGOS data. In our analyses, bird speed refers to ground speed, which in our case, is the point-to-point speeds calculated along a bird's interpolated track line. Although, point-to-point speeds estimated from ARGOS data have the tendency to underestimate the true speeds of petrels that travel along zig-zag flight paths (Pennycuik 1982; Alerstam et al. 1993), our ARGOS filtering and relatively short off-periods in duty-cycling would remove unrealistic maximum flight speeds such as those generated from locations estimated over short time series (i.e., <2 h; Nicholls and Robertson 2007). For our analyses, point-to-point values (and interpolated values between points) provided averaged speeds and directions for correlation with winds. We correlated entire track lines and 8-days serial segments from each bird with QSCAT winds. For the serial segment analyses, the 8-days window provides a minimal time window with sufficient co-location sample size (~10–16 co-locations twice daily) to calculate meaningful vector correlation coefficients along an individual's track line (Breaker et al. 1994). Temporal and spatial autocorrelation effects are expected to be minimal because co-locations are separated by a minimum of ~12 h. Furthermore, because the frequency of co-locations is set by the satellite orbit, and this remains consistent for any tracked seabird, autocorrelation effects are incorporated into the calculation of the single vector correlation coefficient. We determined statistical significance for entire track line correlations among individuals using the resampling technique described earlier for buoy–QSCAT correlation. Because QSCAT winds potentially are autocorrelated over short time-scales (several hours to several days), bootstrapped probability estimates should be examined with caution when near $\alpha = 0.05$ or at when co-location sample size is appreciably large (i.e., bootstrapped P values would tend to underestimate the true values). Lastly, we calculated isotropic, vector-averages and directional standard deviations for incidental wind angles ($\alpha \pm$ SD) experienced by birds following Yamartino (1984). All graphical representations of winds and bird trajectories are depicted using the oceanographic convention.

Results

Vector correlation of buoy and QSCAT winds

RSS rain flagging applied to QSCAT data removed 3–17% of the co-located data (greatest flagging at 46,042, Monterey Bay; Table 1). Our wind flagging applied to QSCAT data removed an additional 6–13% of the co-located data (greatest flagging at 46,063, Point Conception; Table 1). After rain and wind flagging, there remained from 75% of co-located data at station 46,042 (Monterey Bay) to 92% of co-located data at station 51004 (southeast Hawaii; Table 1).

NDBC buoy winds and QSCAT winds show close agreement in magnitude and direction (Fig. 1). For all wind speeds considered, vector correlations r_v^2 ranged from 1.28 at station 46063 (Point Conception) to 1.90 at station 46066 (southeast Aleutians; Table 2). Vector correlations generally were least when buoy winds were 0–5 ms^{-1} and greatest when buoy winds were 10–15 ms^{-1} (exception at station 51004, southeast Hawaii; Table 2).

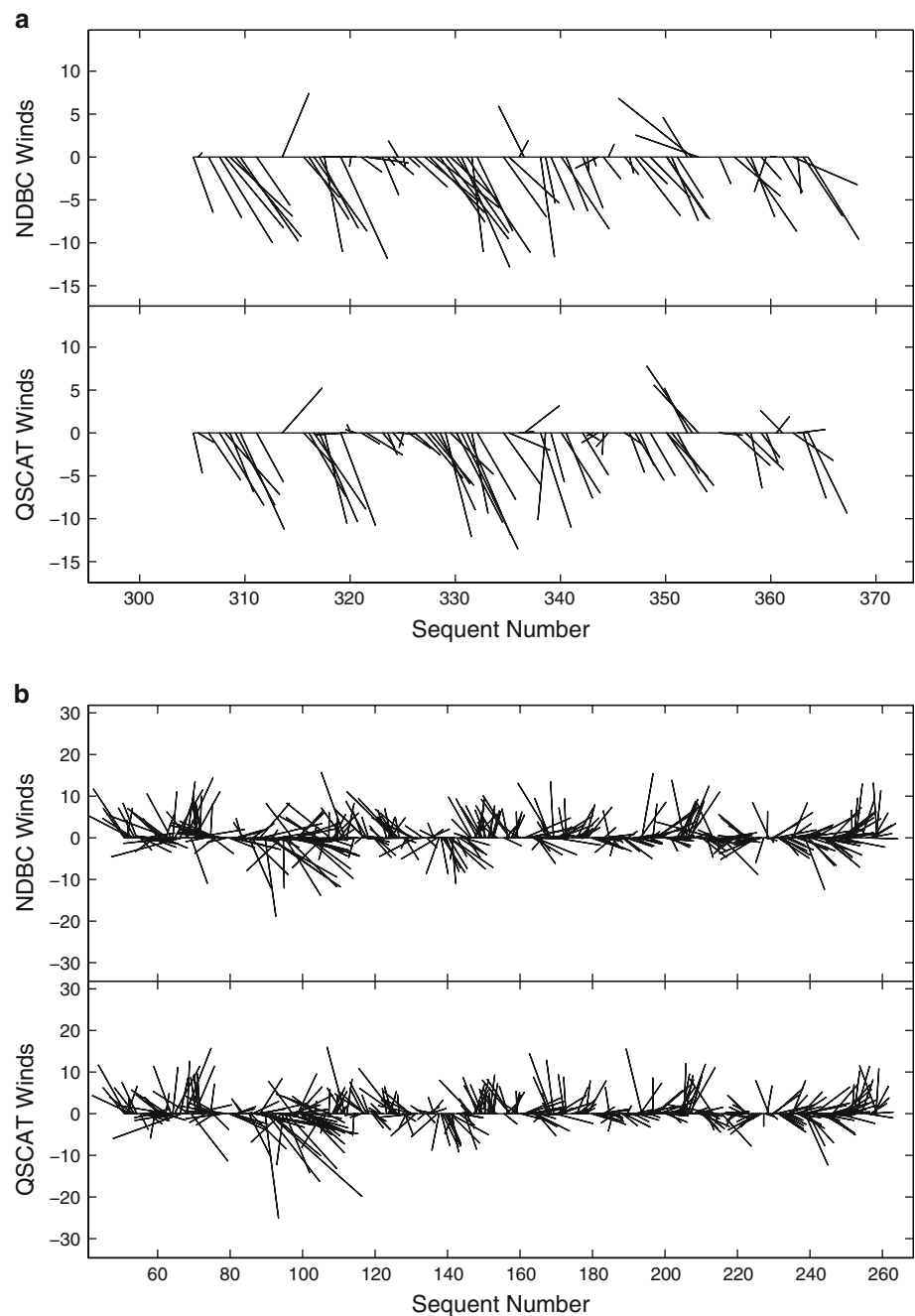
Vector correlation of seabird trajectories and QSCAT winds

The five petrels were tracked for 19–95 days. After filtering, we retained 84–89% of ARGOS location data for hourly interpolation (Table 3). Depending on tracking duration, interpolated bird locations provided 34–123 bird–QSCAT co-locations of which we retained 95–98% for analyses after rain and wind flagging.

Sooty Shearwater #66523 (sub-adult or adult) departed California coastal waters on October 6, 2006, and followed a southwestward migration route toward New Zealand; it turned eastward when winds changed from westward to eastward near 43°S latitude (Fig. 2a). Overall, this individual's movements were significantly correlated with QSCAT winds ($r_v^2 = 0.61$, $P < 0.0001$; Table 4). Maximum 8-days $r_v^2 = 1.25$ occurred October 14–21 as the bird crossed the equatorial Pacific between 8°N and 14°S (Fig. 2a; Table 4). Throughout its track line, the shearwater traveled predominantly with crossing tail-winds ($118^\circ \pm 31^\circ$; Fig. 3a).

Pink-footed Shearwater #64378 (post-breeding adult) departed its colony in the Juan Fernandez Islands, Chile on April 26, 2006. It traveled northward along the Chile–Peru coastline *en-route* to a wintering site along the southern coast of Baja California Sur, Mexico (Fig. 2b). Overall, this individual's movements were significantly correlated with QSCAT winds ($r_v^2 = 0.49$, $P = 0.0054$; Fig. 2b; Table 4). PTT duty-cycling (48-h off-periods) precluded sufficient co-located data (i.e., >10 co-locations per 8-days) to calculate r_v^2 for path segments. This shearwater

Fig. 1 Example stick-plots of co-located winds measured two NDBC buoys and measured by QSCAT: **a** NDBC Buoy 46063 (Point Conception, CA) and **b** NDBC Buoy 46066 (Southern Aleutians, Gulf of Alaska). North is aligned with the y -axis (scaled to wind speed in ms^{-1}), sticks are anchored along $y = 0$ and show the direction and magnitude that winds are blowing, and sequent number corresponds to Julian day



traveled with a variety of quartering tail-winds, crossing winds, and occasional head-winds ($100^\circ \pm 34^\circ$; Fig. 3b).

Hawaiian Petrel #68020 (breeding adult) departed its nesting burrow on Haleakala, Maui, Hawaii on August 9, 2006, and traveled along a counterclockwise loop through the northeast Pacific Ocean before returning to its burrow after 19 days at sea (Fig. 2c). Overall, movements were significantly correlated with QSCAT winds ($r_v^2 = 0.59$, $P < 0.0001$; Fig. 2c; Table 4). Maximum 8-days $r_v^2 = 1.08$ occurred August 12–19 as the bird turned from northwestward to northeastward with changing winds associated with a near-stationary NE Pacific anticyclone (high-

pressure cell; Table 4, Fig. 4a). This petrel traveled predominantly with quartering tail-winds ($120^\circ \pm 24^\circ$; Fig. 3c).

Grey-faced Petrel #67596 (colony-attending adult, breeding status unknown) departed its colony in the Alderman Islands, New Zealand on July 17, 2006, to travel throughout portions of the southwest Pacific, Tasman Sea, and East Australian coastline (Fig. 2d). Overall, this individual's movements were significantly correlated with QSCAT winds ($r_v^2 = 0.55$, $P < 0.0001$; Fig. 2d; Table 4). Maximum 8-days $r_v^2 = 1.36$ occurred August 20–27, while it transited counterclockwise around an

Table 2 Vector correlation (Crosby et al. 1993) for winds measured at Pacific NDBC buoys and co-located winds derived from the SeaWinds scatterometer onboard the QuikSCAT spacecraft

Buoy	Location	All wind speeds	Binned wind speeds			
			0–5 ms ⁻¹	5–10 ms ⁻¹	10–15 ms ⁻¹	>15 ms ⁻¹
46063	Point Conception, CA	1.28	–	1.33	–	–
46066	Southern Aleutians, AK	1.90	1.66	1.92	1.93	–
46042	Monterey bay, CA	1.31	0.80	1.41	1.56	–
46059	Offshore, CA	1.75	1.55	1.70	1.86	–
51004	Southeast, HI	1.72	1.42	1.64	1.27	–
51028	Christmas Island	1.68	1.33	1.61	–	–

Values are presented for all wind speeds and binned wind speeds: 0–5 ms⁻¹, 5–10 ms⁻¹, 10–15 ms⁻¹, and >15 ms⁻¹. Values were calculated only for paired vector sets with >29 pairs; cells with pairs <30 are indicated by a dash. All vector correlations (r_v^2) are significant ($P < 0.0001$)

Table 3 Summary satellite tracking data for five procellariiform seabirds

Species	PTT ID	PTT Maker ^a	Duty cycle, hours (on:off)	Start	End	Days tracked	Total locations	Locations retained (%)
SOSH	66523	Sirtrack	10:14	9/24/2006	11/8/2006	47	464	412 (89)
PFSH	64378	Microwave	10:48	4/26/2006	7/30/2006	95	324	282 (87)
HAPE	68020	Microwave	Continuous	8/9/2006	8/28/2006	19	530	447 (84)
GFPE	67596	Sirtrack	2:2	7/17/2006	9/26/2006	72	773	673 (87)
BFAL	36338	Sirtrack	Continuous	7/26/2004	9/16/2004	52	1395	1199 (86)

^a Sirtrack, Ltd, Havelock North, New Zealand: KiwiSat 202, Sirtrack, Ltd, 31 g (*SOSH* and *GFPE*); 54 g (*BFAL*). Microwave Telemetry, Columbia, MD, USA: Solar PTT 18 g (*PFSH*) and Solar PTT 12 g (*HAPE*)

anticyclone (Table 4, Fig. 4b). This petrel traveled predominantly with quartering tail-winds, occasionally with crossing winds, and occasionally with tail-winds ($129^\circ \pm 23^\circ$; Fig. 3d).

Black-footed Albatross #36338 (non-breeding season, breeding-age [plumage class 3; Hyrenbach 2002]) was tracked from the California Current to the central North Pacific. Overall this individual's track line was significantly correlated with QSCAT winds ($r_v^2 = 0.31$, $P < 0.0001$; Fig. 2e; Table 4). Maximum 8-days $r_v^2 = 1.34$ occurred August 18–24 as the bird transited across the central Gulf of Alaska through two cyclones (low-pressure cells). During this segment, this individual traveled through a northeastward-propagating 1,004-mb cyclone, across a weak ridge of high pressure, then accelerated toward a second, stronger 982-mb cyclone. The albatross passed through this second cyclone then turned 90° southward coincident with a shift in wind direction as the bird reached the cyclone's leeward side (Fig. 5). The albatross then remained in a 3×10^6 km² region south of the Aleutian islands where it experienced variable wind directions and displayed lesser 8-days r_v^2 values (Fig. 2e). This albatross traveled predominantly with quartering tail-winds, occasionally with crossing winds and crossing head-winds, and occasionally with tail-winds ($115^\circ \pm 30^\circ$; Fig. 3e).

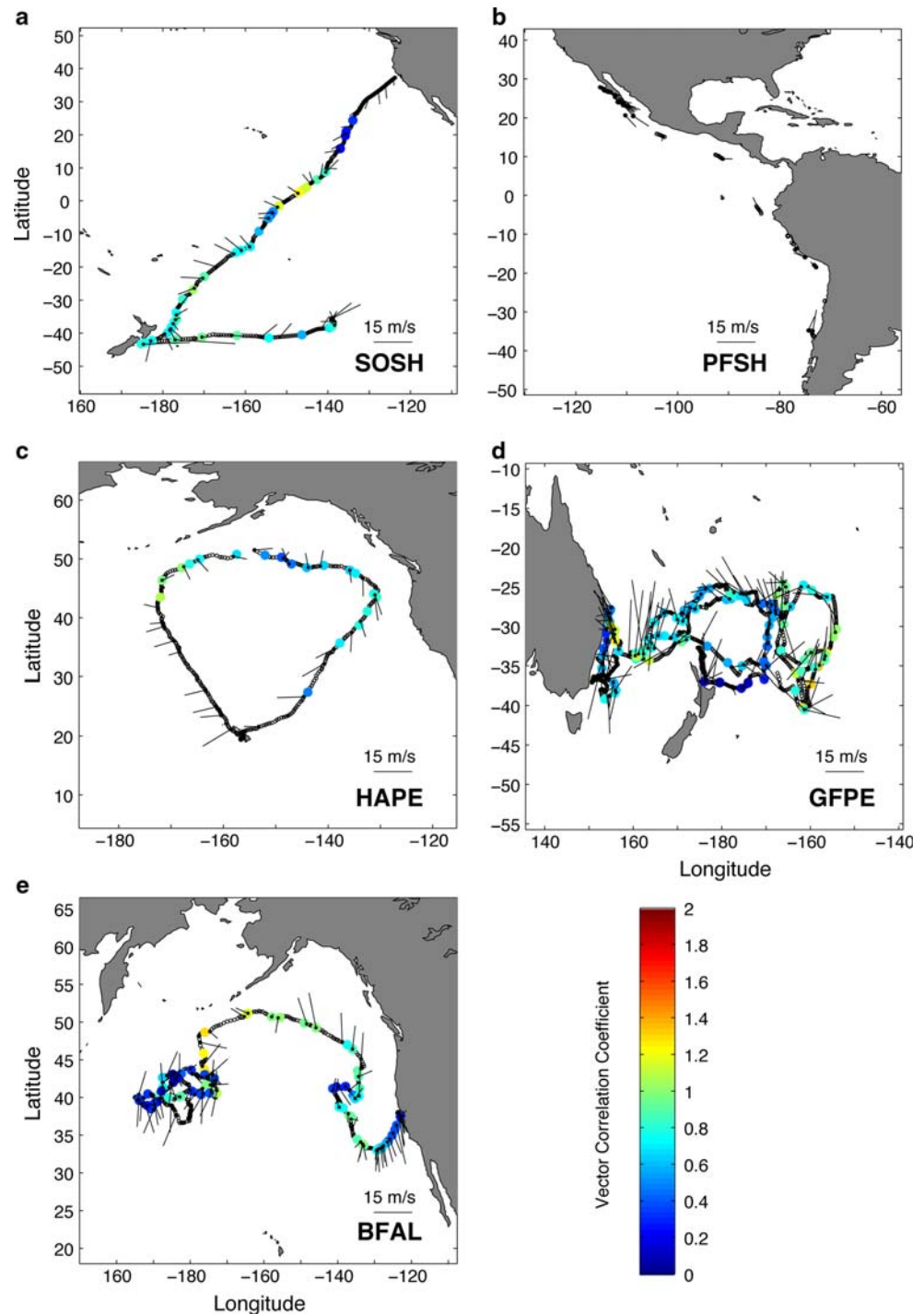
Discussion

Buoy–QSCAT wind correlations

Vector correlations (range in $r_v^2 = 1.28$ – 1.90) between co-located winds measured at buoys and by SeaWinds on QuikSCAT in our study are consistent with Freilich and Dunbar (1999) who report vector correlations r_v^2 of <1.4 (coastal buoy locations), 1.6–1.8 (offshore California, Washington, and Hawaii), and >1.8 for offshore buoys located in the NE Pacific. Vector correlations in their study were computed using winds (within 50 km) measured by the similar NASA scatterometer during the brief NSCAT-mission preceding the launch of the SeaWinds scatterometer. Sánchez et al. (2007) observed r_v^2 ranging from 1.33 to 1.61 among land-based anemometers along the Iberian Peninsula, Portugal and co-located QSCAT data (within 80 km of station).

The greatest relative percentage of rain flagging at Monterey Bay buoy 46042 likely resulted from the dense marine layer (coastal fog) off the central California coastal region and the conservative flagging employed by RSS, rather than actual rainfall. The greatest relative wind flagging and lowest buoy–QSCAT vector correlation occurred at the Point Conception Buoy 46063 located 27 km from shore and in a region with a wind field that is modified by

Fig. 2 Track lines for five procellariiform seabirds; open circles are hourly interpolated locations, sticks show co-located wind speeds and directions from QSCAT (sticks are anchored at the birds' location and show the direction and magnitude that winds are blowing), and colored circles denote 8-days running vector correlation values (*color bar*) between bird movements and QSCAT winds (plotted on the location corresponding to the middle of the time window): **a** Sooty Shearwater (*SOSH*), **b** Pink-footed Shearwater (*PFSH*), **c** Hawaiian Petrel (*HAPE*), **d** Grey-faced Petrel (*GFPE*), and **e** Black-footed Albatross (*BFAL*)



coastal mountain topography. Freilich and Dunbar (1999) also reported lowest vector correlations among coastal buoy stations where small-scale wind variability was expected to be greatest. We suspect that lower relative vector correlation at the southeast Hawaii buoy 51004 results from increased small-scale variability in wind speeds and directions detected by buoys with associated downdrafts resulting from virga in the wake of localized microbursts. Unlike the case in Monterey Bay, the rain

flagging method employed by RSS for QSCAT data may not be as sensitive to such small-scale events that would be detected more accurately by buoy-based anemometers.

Petrel–QSCAT wind correlations

Our method for integrating petrel movements with QSCAT winds provides a convenient way to measure how seabirds travel in association with ocean winds. Movements

Table 4 Summary of QSCAT wind data and procellariid co-locations

Species	PTT ID	Co-locations	Rain flags	Wind flags	Co-locations retained (%)	r_v^2	P value ^a	r_v^2 max (n) ^b	Angular difference ^c
SOSH	66523	56	0	2	54 (96)	0.61	<0.0001	1.25 (10)	118 ± 31
PFSH	64378	41	0	3	38 (93)	0.49	0.0054	–	100 ± 34
HAPE	68020	36	0	2	34 (94)	0.59	<0.0001	1.08 (15)	120 ± 24
GFPE	67596	126	0	3	123 (98)	0.55	0.0001	1.36 (13)	129 ± 23
BFAL	36338	96	0	3	93 (97)	0.31	<0.0001	1.34 (14)	115 ± 30

Shown are species (*SOSH* Sooty Shearwater, *PFSH* Pink-footed Shearwater, *HAPE* Hawaiian Petrel, *GFPE* Grey-faced Petrel, *BFAL* Black-footed Albatross), PTT ID, total number of bird–QSCAT co-locations, number of rain and wind flags, total number of co-locations retained (percent), complete track line vector correlation coefficient r_v^2 (Crosby et al. 1993; bold values denote significance), bootstrapped P value for r_v^2 used to assess significance, maximum 8-days vector correlation coefficient r_v^2 max (n = sample size), and the complete track line angular difference (±SD) between co-located winds with respect to each bird’s traveling direction (incidental to birds and irrespective of birds’ side). Dash indicates insufficient co-location data to calculate meaningful r_v^2 value

^a Bootstrapped P value for complete track line r_v^2

^b Maximum correlation coefficient calculated along moving 8-days window throughout each individual’s track line

^c We consider the incidental angle of the wind as it touches a bird traveling in the forward direction such that wind angles 105–165° (winds from the bird’s right) are equivalent to winds 195–255° (winds from the bird’s left); throughout we refer to the incidental angles ranging from 0 to 180° (see Fig. 3 for graphical explanation)

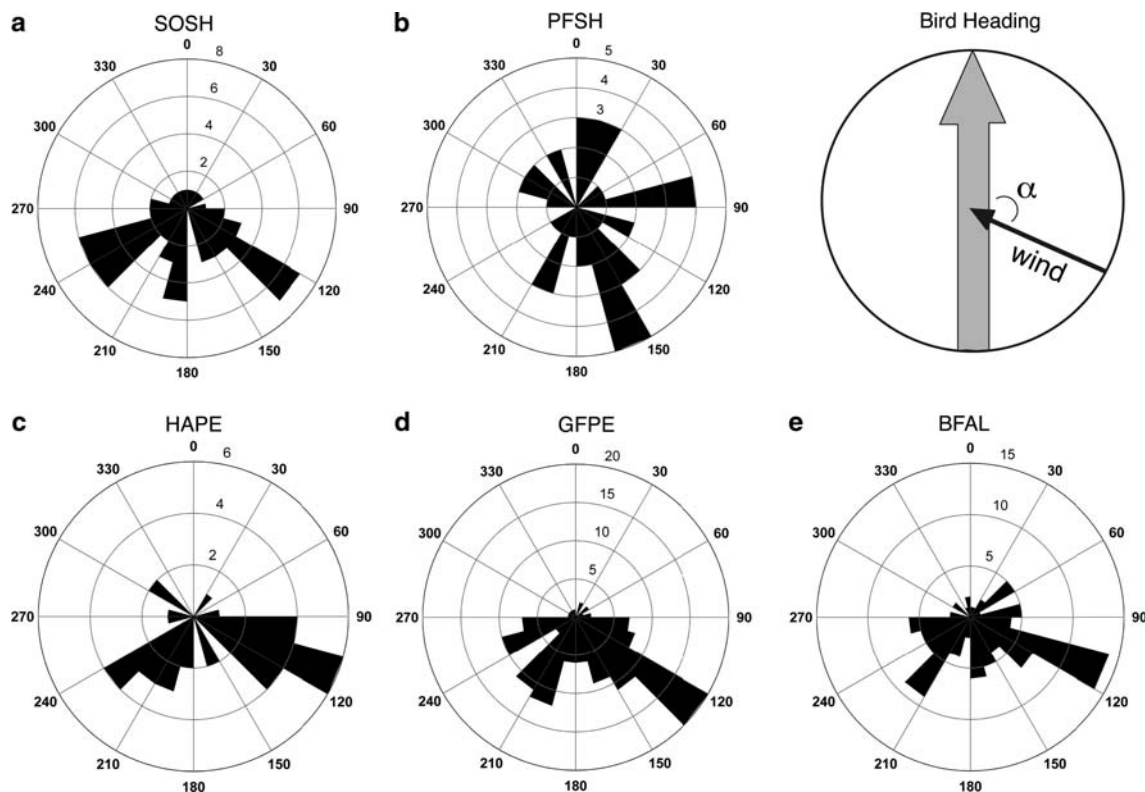


Fig. 3 Rose-plots showing the frequency of co-located QSCAT wind directions (α) relative to each bird’s trajectory for five procellariiform seabirds: **a** Sooty Shearwater (*SOSH*), **b** Pink-footed Shearwater

(*PFSH*), **c** Hawaiian Petrel (*HAPE*), **d** Grey-faced Petrel (*GFPE*), and **e** Black-footed Albatross (*BFAL*). Spokes show frequency of wind direction in bins of 15°

constituting the entire track lines among all five petrels examined were significantly correlated with co-located winds measured by satellite-based scatterometry. Vector correlation (r_v^2) values calculated over an individual’s entire track line generally were less than the greatest values

calculated along serial multi-day sections (i.e., 8-days windows used in this study).

Both the non-breeding *GFPE* and *BFAL* displayed lesser r_v^2 8-days values within spatially concentrated areas separated by path segments characterized by relatively greater

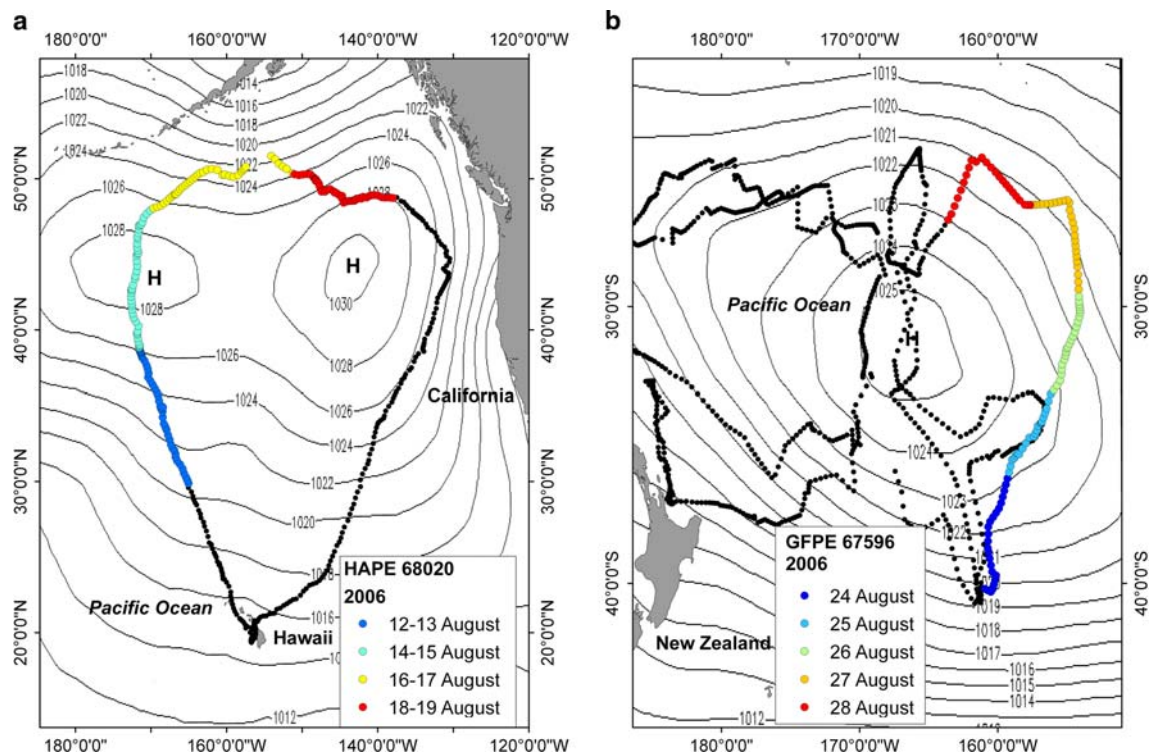


Fig. 4 Track line segments corresponding to maximum 8-days vector correlations for (a) Hawaiian Petrel and (b) Grey-faced Petrel. Synoptic sea-level pressure isopleths (mb) averaged over same period as colored track line segments are shown and reveal location of northern and southern hemisphere anticyclones (high-pressure cells).

r_v^2 values (Fig. 2d, e). The GFPE traveled from a colony in northeastern New Zealand to concentrate activity within a well-defined hotspot area for this species off the east coast of Australia (Fig. 2d; MacLeod et al. 2008). The BFAL displayed aggregated locations and lesser r_v^2 values within two regions: off central California and in the central northwestern Pacific; both areas were separated by a path segment with relatively greater r_v^2 values (Fig. 2e).

High variability among serial vector correlation windows for the individual petrels in this study [ranging from low values (0.05) to relatively high values (1.36)] indicate that correlated wind- and movement-related ‘events’ may exist for seabirds traveling at sea. This pattern in serial trend data was addressed by Crosby et al. (1993) who described ‘wind-event’ scaling as oscillating periods where vector correlation achieves peak values. Many pelagic seabirds that forage in a hierarchical system, where prey resources are patchily distributed at multiple spatial scales (Fauchald 1999), adopt ranging strategies that alternate between spatially concentrated movements (i.e., area-restricted-searching [ARS] and longer-range directed movements between ARS areas). These movement patterns are especially well documented during the breeding season when adults provisioning chicks commute between their colonies and

Winds (birds) flow (travel) clockwise (counterclockwise) in the northern (southern) hemisphere, respectively. Averaged daily sea surface pressures are available from <http://www.esrl.noaa.gov/psd/data/gridded/data.ncep.html>, accessed October 14, 2009

distant foraging areas (Weimerskirch et al. 1997; Hyrenbach et al. 2002; Pinaud and Weimerskirch 2005, 2007; Suryan et al. 2006, 2008). Suryan et al. (2006), however, found interpretation of ARS behavior among non-breeding Short-tailed Albatrosses confusing because albatross movements can be particularly affected by wind speed (see also Jouventin and Weimerskirch 1990). We suggest moving-window vector correlation or comparison between ARS segments and non-ARS segments can provide additional information useful for future interpretations of ARS behaviors and habitat selection among seabirds. For example, to what degree do presumed key foraging areas—based on either reduced flight speeds and increased turning rates (Weimerskirch et al. 1997; Hyrenbach et al. 2002) or ARS behaviors (Pinaud and Weimerskirch 2005, 2007)—also depend on correlated versus non-correlated movements with ocean winds? Further analyses could also examine variable window durations to help resolve temporal scaling in seabird movement–ocean wind correlations.

The five individual petrels in this study all flew predominantly with crossing tail-winds (105–165°). In the eastern tropical Pacific Ocean, Spear and Ainley (1997a,b) observed Procellariiformes as a group primarily flew with crossing winds (70–110°, relative to bird headings) with

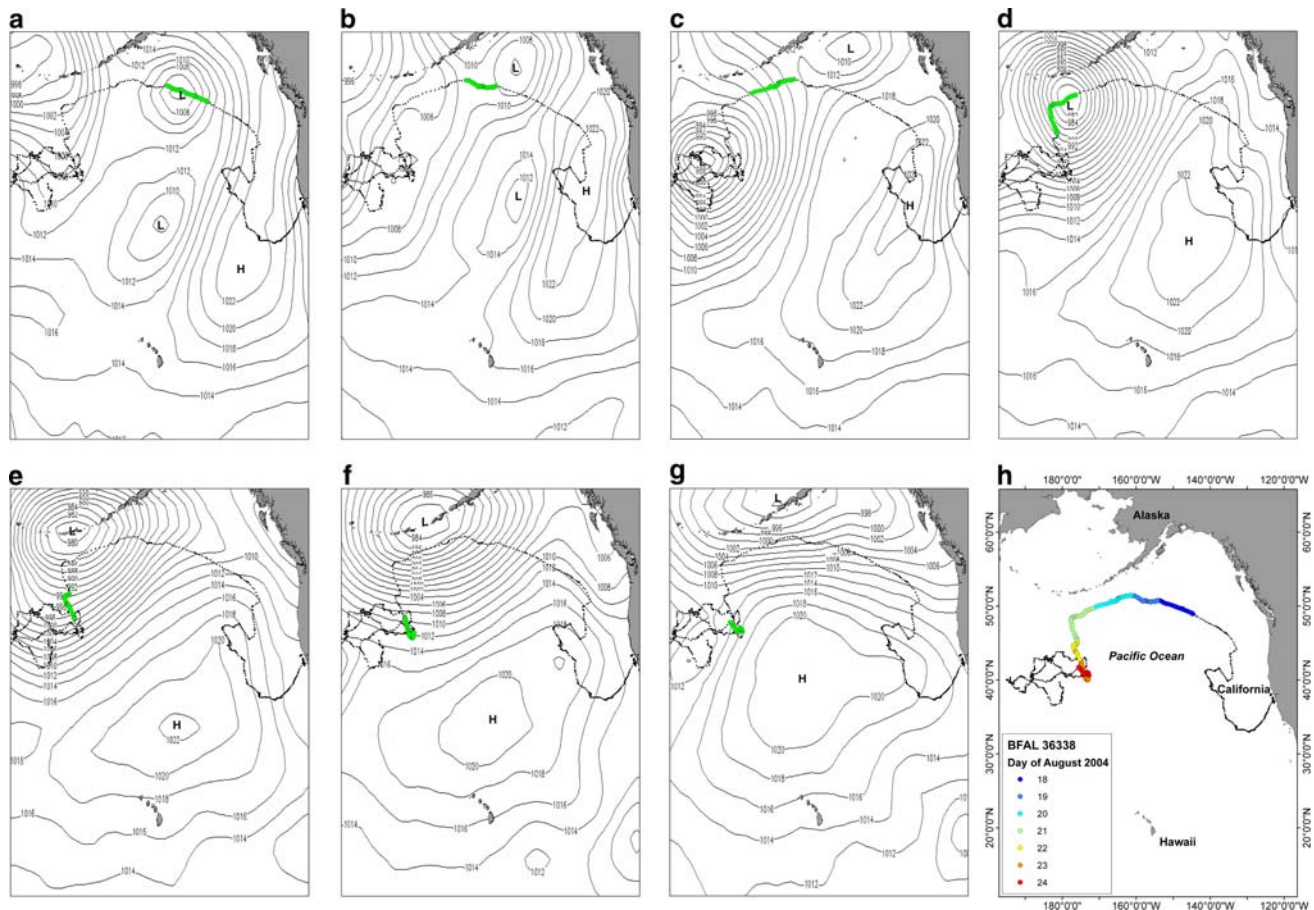


Fig. 5 Synoptic, daily averaged sea level pressure isopleths (mb) and daily track line segments for a Black-footed Albatross during the 8-day period of maximum vector correlation with co-located winds (7 days are shown). Colored dots in lower right inset (h) depict the bird's hourly locations on a given day between 18 and 24 August 2004. **a** Day 1: the bird flies near the core of the first weak cyclone; **b** Day 2: bird travels across a weak ridge of high pressure; **c** Day 3: approaches with quartering tail winds the north side of a stronger

northeastward progressing cyclone, then on **d** Day 4: travels near the core of the second cyclone then abruptly turns south as the wind direction changed following the northeastward progression of the second cyclone (see Fig. 2e); **e–g** Days 5–7: bird moves south away from the cyclone to slow-down within a weak ridge of high pressure. Averaged daily sea surface pressures are available from <http://www.esrl.noaa.gov/psd/data/gridded/data.ncep.html>, accessed 14 October 2009

incidence of headwind flight positively correlated with wing loading and incidence of tailwind flight negatively related to aspect ratio. Within our group, the HAPE and GFPE have high wing aspect ratios and the least wing loading. The shearwaters have intermediate wing loadings and lower aspect ratios. The BFAL deviates from the group in having both greater wing loading and higher aspect ratio. Our results show that the two *Pterodroma* petrels and the albatross traveled most frequently with quartering tail-winds, and generally avoided headwinds, albeit the albatross occasionally traveled with slightly more crossing to head-winds. With proportionately larger wings, the large gadfly petrels (e.g., HAPE and GFPE) appear to make relatively better use of tail-wind and cross-wind force than larger-bodied albatrosses (Spear and Ainley 1997b). Unlike the petrels and albatross, both shearwaters were engaged in directed movements associated with long-distance

migration. The SOSH traveled more so with crossing winds and occasional head-winds and the PFSH traveled more frequently than the others with head-winds and tail-winds. The pattern displayed by the PFSH may have resulted from inclusion in our analyses of an extended wintering period off the coast of Baja California, Mexico where, in order to remain over the narrow continental shelf, the PFSH would either fly into or against the prevailing northwesterly winds.

Our results also agree with previous telemetry-based studies that comment on how seabirds (restricted almost exclusively to Wandering Albatrosses) fly with winds. Using wind direction derived from sea-level pressure models, Jouventin and Weimerskirch (1990), found Wandering Albatrosses (*Diomedea exulans*) outfitted with satellite transmitters departed their colony with crossing tail-winds (112–157°) and returned generally with crossing

head-winds (68–113°). Our observation that the BFAL tended to avoid headwinds may relate to this bird's non-breeding status when directed movements are not influenced by the need to commute between foraging areas and a colony. Movements during the non-breeding season should be more influenced by wind direction and strength rather than by the need to commute to a specific area or colony local. Both petrels, the SOSH, and BFAL all show directional (and ground speed) changes associated with changing winds encountered (i.e., path segments with relatively great vector correlations, Fig. 2). These results are consistent with Weimerskirch et al. (1993) who observed breeding Wandering Albatrosses changed course when wind directions changed in order to maintain use of crossing tail-winds during long, looping foraging trips. Reinke et al. (1998) used winds derived from modeled sea-level pressures and found similar results as Weimerskirch et al. (1993) for an individual Wandering Albatross; the bird traveled closer in angle to winds of moderate speeds than to high winds (i.e., opposite to the observations of Alerstam et al. 1993). The SOSH in our study (Fig. 2a) traveled closer in angle with relatively greater tail-winds after reaching New Zealand, consistent with observations of albatross by Alerstam et al. (1993). The tail-winds experienced by the SOSH at 40–50°S likely were strong enough to overcome this species' observed propensity for avoiding relatively weaker tailwinds at subtropical latitudes (Spear and Ainley 1997a).

To our knowledge, Suryan et al. (2006, 2008) is the only author to have evaluated QSCAT winds along albatross track lines. More recently, Felicísimo et al. (2008) and González-Solís et al. (2009) used QSCAT winds to calculate and map model-derived hypothetical “minimum wind cost trajectories” for three migrating shearwaters: Cory's (*Calonectris diomedea*), Manx (*Puffinus puffinus*), and Cape Verde (*C. edwardsii*). Their models, however, are based on passive particle drift and assumed a minimum flight cost (arbitrary units) when birds traveled directly with tailwinds, despite observations that, in most conditions, similar shearwater species tended to avoid tailwinds (e.g., Spear and Ainley 1997a). The propensity for petrels to avoid tailwinds also has been observed by others. When traveling >100 km day⁻¹, Short-tailed Albatrosses (*Phoebastria albatrus*) traveled downwind (135–235° incidental angle relative to bird's trajectory), both Laysan (*Phoebastria immutabilis*) and Black-footed Albatrosses traveled at 90° relative to the wind, but breeding Waved-albatrosses (*Phoebastria irrorata*) traveled within 45° of the wind (both head- and tail-winds; Suryan et al. 2008).

Given significant correlations with ocean winds in this study and observations described in previous studies, seasonally and spatially predictable winds associated with sea-level pressure patterns over the oceans (e.g., blocking

anticyclones; Higgins and Schubert 1994; Wiedenmann et al. 2002) undoubtedly affect seabird movements over large expanses of open ocean. Winds associated with slower-moving, anticyclonic (high-pressure center) and faster propagating, less stationary cyclonic (low pressure center) circulation likely are important for determining in part the at-sea distribution and long-range trajectories among the Procellariiformes. We suggest vector correlation can provide quantitative insight into how ocean winds—determined by the sea-level atmospheric pressure topography (i.e., cyclones and anticyclones)—significantly affect the movement paths of birds transiting large expanses of the world's oceans. For example, the HAPE tracked during August 2006, achieved a maximum vector correlation while traveling eastward (i.e., clockwise) to circumnavigate a slow-moving North Pacific 1,030-mb anticyclone (high-pressure system; Fig. 4a). We observed a similar pattern in the related GFPE off New Zealand. Maximum vector correlation for this individual occurred also while circumnavigating (i.e., counter-clockwise) a 1,025-mb anticyclone northeast of New Zealand (Fig. 4b). Nicholls et al. (1997) and Murray et al. (2002) speculated that non-breeding Wandering Albatrosses used southern circum-polar winds associated with weather systems between 30 and 50°S to reach any area within this latitudinal band; however, there are no quantitative environmental analyses presented to support their idea. Jouventin and Weimerskirch (1990) observed Wandering Albatrosses occasionally limited their movements and were “trapped” by slack winds (<5 ms⁻¹) for 1–7 days within near-stationary anticyclones. Murray et al. (2003a, b) observed Wandering Albatrosses circumnavigated cyclones when traversing large regions of the Southern Ocean. Blomqvist and Peterz (1984) correlated the occurrence of several seabirds [including two petrels: Sooty Shearwater and Northern Fulmar (*Fulmarus glacialis*)] off Sweden with eastward-propagating cyclones and proposed a causal model based on cyclonic wind conditions, wave patterns, and flight behavior to explain the generalized clockwise movements of birds over the Baltic Sea. Consistent with the observations of Murray et al. (2003a, b), but different from our observations of a single BFAL (Fig. 5), they suggested that seabirds on the open ocean should avoid flying into cyclone centers.

SeaWinds data are available from July 1999 to the present. The relatively long-term availability of scatterometer-derived ocean winds allows researchers to revisit archived seabird satellite tracking data (BirdLife International 2004). Unfortunately, SeaWinds on QuikSCAT has surpassed its operational life (estimated at 5 years from launch in 1999) and a replacement sensor has yet to be identified when the current unit fails (Witze 2007). Analyses presented herein also are suitable for wind data such

as those generated by the NOAA National Centers for Environmental Prediction (e.g., NCEP_Reanalysis 2; Kanamitsu et al. 2002; see <http://www.esrl.noaa.gov/psd/>, accessed October 14, 2009) or other similar data sets. These data extend the ability to examine vector correlation to seabird tracking studies that occurred before 1996 when the first scatterometer was deployed (NSCAT). Such model-derived data, however, although available at greater temporal frequency (i.e., 4-h intervals), do not retain the same spatial accuracy (2.5° pixel) as scatterometer-derived winds (0.25° pixel). Methods presented herein provide a standardized approach for quantifying movements associated with ocean-surface winds that can provide additional insight into ranging behaviors. Researchers, however, should be aware of several potential limitations. Even relatively low correlation coefficients can be statistically significant when co-location sample sizes are appreciably high. Interpretations of comparisons should be based on vector correlation coefficients that are calculated from a sufficient number, and preferably, similar sample sizes of co-located data. Because locally observed winds are determined at 0600 and 1800 local time, analyses involving species or individuals that have strong diurnal behavioral patterns related to feeding or traveling may be limited. Additionally, for species that travel very close to shore (<25 km from the coastline) it may be difficult or impossible for QSCAT to resolve wind speed and direction accurately. Lastly, it is important to recognize that petrels also make use of waves (both wind waves and ground swells) for flight at the ocean's surface (Blomqvist and Peterz 1984; Pennycuik 2002; Suryan et al. 2008); although we focused here on the correlation of petrel movements with surface winds, future analyses may benefit by examining vector correlations with wave parameters such as amplitude, period, and direction (see <http://polar.ncep.noaa.gov/waves/products.html>, accessed October 15, 2009). Future analyses relating seabird movements with ocean winds can provide insight into the effects of environmental changes on ocean wind fields (Parrish et al. 2000; Vecchi et al. 2006). Lastly, vector correlation techniques herein are not limited to seabirds and wind—they also can be used to examine relationships and test hypotheses among any marine vertebrate that moves through waters where currents are measured and/or can be derived from models (Brooks 2005), remote measurements (i.e., geostrophic flow derived from radar altimetry: Ream et al. 2005; Hawkes et al. 2006; Lambardi et al. 2008), or drifters (Bentivegna et al. 2007).

Acknowledgments We thank L. Breaker and E. McPhee-Shaw for enthusiastic discussions and useful contributions. P. Hodem and K. D. Hyrenbach provided PFSH data, P. Lyver provided GFPE data; BFAL data were supplied as part of a collaborative effort on behalf of *Oikonos Ecosystem Knowledge*, HAPE data were supplied as part of a

collaborative effort on behalf of US Geological Survey (USGS) Western Ecological Research Center, D. G. Ainley (HT Harvey and Associates), H. Friefeld (US Fish and Wildlife Service), C. Bailey and J. Tamayose (Haleakala National Park), and J. Penniman (Hawaii Department of Land and Natural Resources); and SOSH data were supported in part by Moss Landing Marine Labs, USGS, and UC Santa Cruz Tagging of Pacific Pelagics. C. MacLeod kindly provided assistance with programming in R. QuikSCAT. Data are produced by remote sensing systems and sponsored by the NASA Ocean Vector Winds Science Team. QSCAT data are available at www.remss.com. Previous drafts of this paper benefited from comments and suggestions provided by H. Moller, D. G. Ainley, J. Yee, K. Phillips, and four anonymous reviewers. The use of trade, product, or firm names in this publication is for descriptive purposes only and does not imply endorsement by the US Government.

References

- Abrams RW (1985) Environmental determinants of pelagic seabird distribution in the African sector of the southern ocean. *J Biogeography* 12:473–492
- Acosta CA, Matthews TR, Butler MJ IV (1997) Temporal patterns and transport processes in recruitment of spiny lobster (*Panulirus argus*) postlarvae to south Florida. *Mar Biol* 129:79–85
- Ainley DG (1977) Feeding methods in seabirds: a comparison of polar and tropical nesting communities in the eastern Pacific ocean. In: Llano GA (ed) Adaptations within Antarctic ecosystems. Proceedings of the 3rd SCAR symposium on Antarctic Biology. Smithsonian Institution, Washington, pp 669–685
- Alerstam T, Gudmundsson GA, Larsson B (1993) Flight tracks and speeds of antarctic and atlantic seabirds: radar and optical measurements. *Phil Trans Biol Sci* 340:155–167
- Aparna M, Shetye SR, Shankar D, Sheno SS (2005) Estimating the seaward extent of sea breeze from QuikSCAT scatterometry. *Geophys Res Lett*. doi:10.1029/2005GL023107
- Ballance LT, Pitman RL, Reilly SB (1997) Seabird community structure along a productivity gradient: importance of competition and energetic constraint. *Ecology* 78:1502–1518
- Bentivegna F, Valentino F, Falco P, Zambianchi E, Hochscheid S (2007) The relationship between loggerhead turtle (*Caretta caretta*) movement patterns and Mediterranean currents. *Mar Biol* 151:1605–1614
- BirdLife International (2004) Tracking ocean wanderers: the global distribution of albatrosses and petrels. Results from the Global Procellariiform Tracking Workshop, 1–5 September, 2003, Gordon's Bay, South Africa; Cambridge, UK: BirdLife International. Available via http://www.birdlife.org/action/science/species/seabirds/tracking_ocean_wanderers.pdf. Accessed 23 Feb 2009
- Blomqvist S, Peterz M (1984) Cyclones and pelagic seabird movements. *Mar Ecol Prog Ser* 20:85–92
- Breaker LB, Gemmill WH, Crosby DS (1994) The application of a technique for vector correlation to problems in meteorology and oceanography. *J Appl Met* 33:1354–1365
- Breaker LB, Gemmill WH, deWitt PW, Crosby DS (2003) A curious relationship between the winds and currents at the western entrance of the Santa Barbara Channel. *J Geophys Res Lett* 108. doi:10.1029/2002JC001458
- Breckling J (1989) The analysis of directional time series: applications to wind speed and direction. Lecture notes in Statistics, vol 61. Springer, New York
- Brooks L (2005) Abundance and tidal movements of green turtle (*Chelonia mydas*) in B.C.S., Mexico Unpublished M.Sc. Thesis, San Jose State University, Moss Landing Marine Laboratories, 116 pp

- Burger AE, Shaffer SA (2008) Application of tracking and data-logging technology in research and conservation of seabirds. *Auk* 125:253–264
- CLS (2007–2008) Argos User's Manual. Available via http://www.argos-system.org/html/userarea/manual_en.html. Accessed 23 Feb 2009. 64 pp
- Coyne MS, Godley BJ (2005) Marine satellite tracking and analysis tool (STAT): an integrated system for archiving, analyzing and mapping animal tracking data. *Mar Ecol Prog Ser* 301:1–7
- Crosby DS, Breaker LC, Gemmill WH (1993) A proposed definition for vector correlation in geophysics: theory and application. *J Atm Ocean Tech* 10:355–367
- Croxall JP, Silk JRD, Phillips RA, Afanasyev V, Briggs DR (2005) Global circumnavigations: tracking year-round ranges of non-breeding albatrosses. *Science* 307:249–250
- Ebuchi N, Graber HC, Caruso MJ (2002) Evaluation of wind vectors observed by QuikSCAT/SeaWinds using ocean buoy data. *J Atm Ocean Tech* 19:2049–2062
- Fauchald P (1999) Foraging in a hierarchical patch system. *Amer Nat* 153:603–613
- Feliciísimo AM, Munõz J, González-Solís J (2008) Ocean surface winds drive dynamics of transoceanic aerial movements. *PLoS ONE* 3(8): e2928. doi:10.1371/journal.pone.0002928
- Freilich MH, Dunbar RS (1999) The accuracy of the NSCAT 1 vector winds: comparisons with the National Data Center Buoys. *J Geophysical Res Let* 104:11231–11246
- Freitas C, Lydersen C, Fedak MA, Kovacs KM (2008) A simple new algorithm to filter marine mammal Argos locations. *Mar Mam Sci* 24:315–325
- Furness RW, Bryant DM (1996) Effect of wind on field metabolic rates of breeding Northern Fulmars. *Ecology* 77:1181–1188
- González-Solís J, Feliciísimo A, Fox JW, Afanasyev V, Kolbeinsson Y, Muñoz J (2009) Influence of sea surface winds on shearwater migration detours. *Mar Ecol Prog Ser* 391:221–230
- Hanson B, Klink K, Matsuura K, Robeson SM, Willmott CJ (1992) Vector correlation: review, exposition, and geographic application. *Annals Assoc Amer Geog* 82:103–116
- Hawkes LA, Broderick AC, Coyne MS, Godfrey MH, Lopez-Jurado LF, Lopez-Suarez P, Merino SE, Varo-Cruz N, Godley BJ (2006) Phenotypically linked dichotomy in sea turtle foraging requires multiple conservation approaches. *Current Biol* 16:990–995
- Higgins RW, Schubert SD (1994) Simulated life cycles of persistent anticyclonic anomalies over the north Pacific: role of synoptic scale eddies. *J Atm Sci* 51:3238–3260
- Hooper JW (1959) Simultaneous equations and canonical correlation theory. *Econometrica* 27:245–256
- Hyrenbach KD (2002) Plumage-based ageing criteria for the Black-footed Albatross *Phoebastria nigripes*. *Mar Ornith* 30:85–93
- Hyrenbach KD, Fernández P, Anderson DJ (2002) Oceanographic habitats of two sympatric North Pacific albatrosses during the breeding season. *Mar Ecol Prog Ser* 233:283–301
- Jouventin P, Weimerskirch H (1990) Satellite tracking of wandering albatrosses. *Nature* 343:746–748
- JPL (2006) QuikSCAT science data product user manual: overview and geophysical data products, Version 3.0, September 2006, D-18053-RevA, Jet Propulsion Laboratory, California Institute of Technology, 91 pp
- Kalnay E, Kanamitsu M, Kistler R, Collins W, Deaven D, Gandin L, Iredell M, Saha S, White G, Woollen J, Zhu Y, Leetmaa A, Reynolds R, Chelliah M, Ebisuzaki W, Higgins W, Janowiak J, Mo K, Ropelewski C, Wang J, Jenne R, Joseph D (1996) The NCEP/NCAR 40-year reanalysis project. *Bull Am Met Soc* 77:437–471
- Kanamitsu M, Ebisuzaki W, Woollen J, Yang S-K, Hnilo JJ, Fiorino M, Potter GL (2002) NCEP-DEO AMIP-II Reanalysis (R-2) Bull Atm Met Soc 1631–1643 Available via <http://www.cpc.ncep.noaa.gov/products/wesley/reanalysis2/kana/rean2-1.htm> Accessed 23 Feb 2009
- Kistler R, Kalnay E, Collins W, Saha S, White G, Woollen J, Chelliah M, Ebisuzaki W, Kanamitsu M, Kousky V, van den Dool H, Jenne R, Fiorino M (2001) The NCEP–NCAR 50-year reanalysis: monthly means CD-ROM and documentation. *Bull Am Met Soc* 82:247–267
- Kundu PK (1976) Ekman veering observed near the ocean bottom. *J Phys Ocean* 6:238–242
- Lambardi P, Lutjeharms JRE, Mencacci R, Hays GC, Luschi P (2008) Influence of ocean currents on long-distance movement of leatherback sea turtles in the Southwest Indian Ocean. *Mar Ecol Prog Ser* 353:289–301
- Liu WT, Tang W (1996) Equivalent neutral wind. Jet Propulsion Laboratory, Pasadena, California Publication 96–17. 20 pp
- MacLeod CJ, Adams J, Lyver P (2008) At-sea distribution of satellite-tracked grey-faced petrels, *Pterodroma macroptera gouldi*, captured on the Ruamaahua (Aldermen) islands, New Zealand. *Papers ProcR Soc Tasmania* 142:73–88
- MathWorks (2007) MATLAB Version 2007. The MathWorks Inc, Natick
- Murray MD, Nicholls DG, Butcher E, Moors PJ (2002) How wandering albatrosses use weather systems to fly long distances 1: an analytical method and its application to flights in the Tasman sea. *Emu* 102:377–385
- Murray MD, Nicholls DG, Butcher E, Moors PJ (2003a) How wandering albatrosses use weather systems to fly long distances 2: the use of eastward-moving cold fronts from Antarctic lows to travel westwards across the Indian ocean. *Emu* 103:59–65
- Murray MD, Nicholls DG, Butcher E, Moors PJ, Walker K, Elliott G (2003b) How wandering albatrosses use weather systems to fly long distances 3: the contributions of Antarctic lows to eastward, southward and northward flight. *Emu* 103:111–120
- NDBC (2003) Handbook of automated data quality control checks and procedures of the National Data Buoy Center, U.S., Department of Commerce, National Oceanic and Atmospheric Administration, National Data Buoy Center, NDBC Technical Document 03–02, 44 pp. Available via <http://www.ndbc.noaa.gov/handbook.pdf> Accessed 25 Nov 2008
- Nicholls DG, Robertson CJR (2007) Assessing flight characteristics for the chatham albatross (*Thalassarche eremita*) from satellite tracking. *Notornis* 54:168–179
- Nicholls DG, Murray MD, Butcher E, Moors P (1997) Weather systems determine the non-breeding distribution of wandering albatrosses over southern oceans. *Emu* 97:240–244
- Parrish RH, Schwing FB, Mendelssohn R (2000) Mid-latitude wind stress: the energy source for climatic shifts in the North Pacific Ocean. *Fish Oceanogr* 9:224–238
- Pennycuik CJ (1982) The flight of petrels and albatrosses (Procellariiformes), observed in South Georgia and its vicinity. *Phil Trans R Soc Lond B* 300:75–106
- Pennycuik CJ (1997) Actual and 'optimum' flight speeds: field data reassessed. *J Exp Bio* 200:2355–2361
- Pennycuik CJ (2002) Gust soaring as a basis for the flight of petrels and albatrosses (Procellariiformes). *Avian Sci* 2:1–12
- Phalan B, Phillips RA, Silk JRD, Afanasyev V, Fukuda A, Fox J, Cury P, Higuchi H, Croxall JP (2007) Foraging behavior of four albatross species by night and day. *Mar Ecol Prog Ser* 340:271–286
- Phillips RA, Silk JRD, Phalan B, Cury P, Croxall JP (2004) Seasonal sexual segregation in two *Thalassarche* albatross species: competitive exclusion, reproductive role specialization or foraging niche divergence? *Proc R Soc Lond B* 271:1283–1291
- Phillips RA, Croxall JP, Silk JRD, Briggs DR (2008) Foraging ecology of albatrosses and petrels from South Georgia: two

- decades of insights from tracking technologies. *Aquatic Conserv: Mar Freshw Ecosyst* 17:S6–S21
- Pinaud D, Weimerskirch H (2005) Scale-dependent habitat use in a long-ranging central place predator. *J Animal Ecol* 74:852–863
- Pinaud D, Weimerskirch H (2007) At-sea distribution and scale-dependent foraging behaviour of petrels and albatrosses: a comparative study. *J Animal Ecol* 76:9–19
- Queiroga H (2003) Wind forcing of crab megalopae recruitment to an estuary (Ria de Aveiro) in the northern Portuguese upwelling system. *Invert Repro Dev* 43:47–54
- R Development Core Team (2007) R: a language and environment for statistical computing. R Foundation for Statistical Computing, Vienna, Austria ISBN 3-900051-07-0. <http://www.R-project.org>. Accessed 23 Feb 2009
- Ream RR, Sterling JT, Loughlin TR (2005) Oceanographic features related to northern fur seal migratory movements. *Deep Sea Res II* 52:823–843
- Reinke K, Butcher EC, Russell CJ, Nicholls DG, Murray MD (1998) Understanding the flight movements of a non-breeding wandering albatross, *Diomedea exulans gibsoni*, using a geographic information system. *Austral J Zool* 46:171–181
- Sachs G (2005) Minimum shear wind strength required for dynamic soaring of albatrosses. *Ibis* 147:1–10
- Sánchez RF, Relvas P, Pires HO (2007) Comparisons of ocean scatterometer and anemometer winds off the southwestern Iberian Peninsula. *Cont Shelf Res* 27:155–175
- Schneider DC (1991) The role of fluid dynamics in the ecology of marine birds. *Ocean Mar Biol Ann Rev* 29:487–521
- Shaffer SA, Costa DP, Weimerskirch H (2001a) Behavioral factors affecting foraging effort of breeding wandering albatrosses. *J Animal Ecol* 70:864–874
- Shaffer SA, Weimerskirch H, Costa DP (2001b) Functional significance of sexual dimorphism in wandering albatross, *Diomedea exulans*. *Funct Ecol* 15:203–210
- Shaffer SA, Tremblay Y, Weimerskirch H, Scott D, Thompson DR, Sagar PM, Moller H, Taylor GA, Foley DG, Block BA, Costa DP (2006) Migratory shearwaters integrate oceanic resources across the Pacific Ocean in an endless summer. *Proc Natl Acad Sci* 103:12799–12802
- Spear LB, Ainley DG (1997a) Flight behaviour of seabirds in relation to wind direction and wing morphology. *Ibis* 139:221–233
- Spear LB, Ainley DG (1997b) Flight speed of seabirds in relation to wind speed and direction. *Ibis* 139:234–251
- Spear LB, Ainley DG (1998) Morphological differences relative to ecological segregation in petrels (Family: Procellariidae) of the southern ocean and tropical Pacific. *Auk* 115:1017–1033
- Spear LB, Ainley DG (1999) Migration routes of sooty shearwaters in the Pacific Ocean. *Condor* 101:205–218
- Spear LB, Nur N, Ainley DG (1992) Estimating absolute densities of flying seabirds using analyses of relative movement. *Auk* 109:385–389
- Spear LB, Ainley DG, Walker WA (2007) Trophic relationships of seabirds in the eastern Pacific Ocean. *Studies in Avian Biol* no 35, 99 pp
- Spruzen FL, Woehler EJ (2002) The influence of synoptic weather patterns on the at-sea behaviour of three species of albatross. *Polar Biol* 25:296–302
- Suryan RM, Sato F, Balogh GR, Hyrenbach KD, Sievert PR, Ozaki K, Tang W (2006) Foraging destinations and marine habitat use of short-tailed albatrosses: a multi-scale approach using first-passage time analysis. *Deep-Sea Res II* 53:370–386
- Suryan RM, Anderson DJ, Shaffer SA, Roby DD, Tremblay Y, Costa DP, Sievert PR, Sato F, Ozaki K, Balogh GR, Nakamura N (2008) Wind, waves, and wing loading: morphological specialization may limit range expansion of endangered albatrosses. *PLoS One* 3(12): e4016. doi: [10.1371/journal.pone.0004016](https://doi.org/10.1371/journal.pone.0004016)
- Tremblay Y, Shaffer SA, Fowler SL, Kuhn CE, McDonald BI, Weise MJ, Bost CA, Weimerskirch H, Crocker DE, Goebel ME, Costa DP (2006) Interpolation of animal tracking data in a fluid environment. *J Exp Biol* 209:128–140
- Vecchi GA, Soden BJ, Wittenberg AT, Held IM, Leetmaa A, Harrison MJ (2006) Weakening of tropical Pacific atmospheric circulation due to anthropogenic forcing. *Nature* 441:73–76
- Warham J (1977) Wing loadings, wing shapes, and flight capabilities of Procellariiformes. *New Zealand J Zool* 4:73–83
- Weimerskirch H, Salamolard M, Sarrazin F, Jouventin P (1993) Foraging strategy of wandering albatrosses through the breeding season: a study using satellite telemetry. *Auk* 110:325–342
- Weimerskirch H, Wilson RP, Lys P (1997) Activity pattern of foraging in the wandering albatross: a marine predator with two modes of prey searching. *Mar Ecol Prog Ser* 151:245–254
- Weimerskirch H, Guionnet T, Martin J, Shaffer SA, Costa DP (2000) Fast and fuel efficient? Optimal use of wind by flying albatrosses. *Proc R Soc Lond B* 267:1869–1874
- Wiedenmann JM, Lupo AR, Mokov II, Tikhonova EA (2002) The climatology of blocking anticyclones for the northern and southern hemispheres: block intensity as a diagnostic. *J Climate* 15:3459–3473
- Wilson JA (1975) Sweeping flight and soaring by albatrosses. *Nature* 257:307–308
- Wilson RP, Grémillet D, Syder J, Kierspel MAM, Garthe S, Weimerskirch H, Christian Schäfer-Neth C, Scolaro JA, Bost CA, Plötz J, Nel D (2002) Remote-sensing systems and seabirds: their use, abuse and potential for measuring marine environmental variables. *Mar Ecol Prog Ser* 228:241–261
- Witze A (2007) Stormy opening to hurricane season. *Nature* 447:514–515
- Yamartino RJ (1984) A comparison of several “single-pass” estimators of the standard deviation of wind direction. *J Climate and Appl Met* 23:1362–1366